Advances in System Identification: Theory and Applications

Damien Guého[1], Puneet Singla[2], Manoranjan Majji[3] and Jer-Nan Juang[4]

Abstract— This paper describes the main features and the most recent developments of system identification in the sense of data-driven modeling of dynamical systems. A brief summary of discrete time-invariant system identification techniques is provided, from the modern work of Gilbert, Kalman and Ho and the introduction of state-space realization, to the most recent developments of the identification of discrete time-varying and nonlinear systems. Important concepts of state-space realization, controllability and observability for linear systems are introduced along with more advanced methods to identify nonlinear dynamics. Numerical examples of varying complexity are considered to demonstrate the capability of the different approaches presented in this paper.

I. INTRODUCTION

System identification as a research topic has attracted some interest over the last decades and has been an important discipline within the automatic control area, robotics, structural engineering, reduced order modeling and model testing [1], [2]. The special purpose of dynamic system identification corresponds to identifying a mathematical model describing a relationship between the input and output of a real system. It is important to distinguish two main basic questions in this context, namely system identification on the one hand and parameter estimation on the other hand. While parameter estimation assumes the existence of a predefined model and uses popular regression techniques to fit the model to time series observations, this paper is mainly concerned with system identification, i.e. with obtaining a mathematical model from time series. However the two have been closely related and parameter estimation historically paved the way for the development of more sophisticated approaches used in system identification.

In the early 19th century more accurate data from observations of the orbits of the planets and the moon became available due to improvements in telescopes, leading to the method of least-squares introduced by Legendre and Gauss. Along with the harmonic analysis of Lagrange and the works of Euler and Fourier, the least-squares technique is considered to be at the origin of data-driven modeling of dynamic systems. Although many results on system identification appears in the statistics (with Fisher in 1912) and econometrics literature in the 20th century, a milestone is reached in 1965 for identification theory in the control community due to the publication of two influential papers [3] and [4]. These papers paved the way for the development of the two mainstream identification techniques that dominate the field today, namely prediction-error identification (based on minimizing a parameter-dependent criterion) and subspace identification (based on projection techniques in Euclidean space).

In their paper, Astrom and Bohlin [3] introduced into the control community the maximum likelihood framework that had been developed by time-series analysts for estimating the parameters of difference equation models [5], [6]. These models, which were known in the statistical literature as ARMA (autoregressive moving average) or ARMAX models (autoregressive moving average with exogeneous inputs), later gave rise to the prediction-error identification framework. On the other hand, Gilbert and Kalman [7], [8] introduced the important principles of realization theory in terms of the concepts of controllability and observability, focusing on linear system identification with a special emphasis on identifying the minimal state space representation to define the subspace over which the system dynamics evolves. They first introduced the concept of state-variable equations which realize the external description via an equivalent internal description of a dynamical system. Whether the analyst or the engineer is interested in the synthesis or the analysis, these equations are an efficient and useful model with which one can proceed to further analysis and optimization. The problem of realization for linear time invariant systems was first stated by Gilbert [7] who provided an algorithm for computing the map transfer function matrix to state-variable differential equations. A second algorithm for the same problem was given at the same time by Kalman [8] using the theory of controllability and observability and requiring linear algebra type computation (state-space models are particularly suitable since they lend themselves to linear algebra techniques, robust numerical simulation, and modern control design methods). A few years later, Ho and Kalman [4] approached this problem from a new viewpoint. They showed that the minimum realization problem is equivalent to a representation problem involving a sequence of real matrices known as Markov parameters (pulse response samples). Minimum realization means a model with the smallest state-space dimension among all possible systems realized that have the same

[1]Damien Guého is a Ph.D. student in the Department of Aerospace Engineering, The Pennsylvania State University, University Park, PA, 16802 djg76@psu.edu

[2]Puneet Singla is a Professor, AIAA Associate Fellow, AAS Fellow, in the Department of Aerospace Engineering, The Pennsylvania State University, University Park, PA, 16802 psingla@psu.edu

[3]Manoranjan Majji is an Assistant Professor, AIAA Associate Fellow, in the Department of Aerospace Engineering, Texas A&M University, College Station, TX, 77840 mmajji@tamu.edu

[4]Jer-Nan Juang is an Affiliate Faculty at Texas AM University, college station, TX, 77840

input-output relations and although several techniques of minimum realization are available in the literature, formal direct application to modal parameter identification for flexible structures was not addressed until 1984.

During the 90s, building upon the initial work by Gilbert and Kalman, several methods have been developed to identify most observable and controllable subspace of the system from given input-output (I/O) data [9]–[13]. Under the interaction of structure and control disciplines, the Eigensystem Realization Algorithm (ERA) [9] was developed for modal parameter identification and model reduction of dynamic systems using test data. The algorithm presents a unified framework for modal parameter identification based on the Markov parameters (i.e., pulse response) making it possible to construct a Hankel matrix as the basis for the realization of a discrete-time state-space model. A few years later at NASA, Juang developed a method for simultaneously identify a linear state-space model and the associated Kalman filter from noisy input-output measurements. Known as the Observer/Kalman Identification Algorithm (OKID) and formulated entirely in the time-domain, it computes the Markov parameters of a linear system, from which the state-space model and a corresponding observer are determined simultaneously [14]–[17]. The method relies on an observer equation to compress the dynamics of the system and efficiently estimate the associated system parameters (Markov parameters). In conjunction with the ERA, the method provides simultaneously both the Markov parameters and the Kalman gain, extracting all the possible information present in the data. The observer at the core of the method was proven to be the steady-state Kalman filter corresponding to the system to be identified. Later, the ERA with Data Correlation (ERA/DC) is developed [10], [18]–[20] and while the ERA is, in essence, a least-squares fit to the pulse response measurements, the ERA/DC involves a fit to the output auto-correlation and cross-correlations over a defined number of lag values.

State-space realizations methods have been shown to work very well for numerical simulations, and for experimental results from structures with modes which are well separated in frequency. The popularity of these methods lies in the simplicity with which the model order can be selected. In general, linear system identification methods are able to capture the main physics as well as the subspace in which the dynamics is evolving. However, linear methods are unable to capture nonlinearities and limitations appear when these state-space methods are applied to complex structures or when a linear description is not accurate enough to fully capture the dynamics within a specific operating range of the system. As contrary to linear system identification, nonlinear system identification problems are still treated mostly on a system-by-system basis with popular methods being Volterra series models [2], [21], [22], global-local learning [23], [24] and neural network (NN) models [25],

[26]. The main essence of nonlinear system identification methods has been to expand the nonlinear unknown function as a linear combination of basis functions or kernels and their amplitude. Many of these methods differ in their choice of basis functions and their learning methodology. Methods like Volterra series approximation utilize Volterra kernels to provide a global approximation of the underlying dynamics while global-local approximation methods merge various local approximations valid in a local region to find a global approximation of the underlying dynamics [23]. More prevalent machine learning methods such as multi-layered NNs (also known as deep NNs) use a composition of nonlinear transformations to approximate the unknown I/O mapping. Each layer of the NN corresponds to one nonlinear transformation which is represented by a linear combination of fixed basis such as sigmoid functions known as neurons or perceptrons. According to Cover and Kolmogorov's theorems [27], [28], multi-layer NNs can serve as universal approximators, but in actuality, they offer no guarantee on accuracy in practice for a reasonable dimensionality (global and distributed approximation can be at the expense of high parametric dimensionality). Furthermore, the learning of parameters for multi-layer NN often involves nonlinear optimization due to composition of multiple nonlinear transformations. All of these methods focus on improving the approximation accuracy by increasing the number of parameters of the models in a brute force manner by increasing the number of basis functions, local models and/or layers of the network. A key issue arises because if one fixes the architecture and basis functions, a given method's ability to approximate a given system's behavior can be deduced only after the learning process is over. Adaptation of the approximation architecture, not simply adjusting weights in a fixed architecture, has emerged as the key to convergence reliability and accuracy. Therefore, approximation capabilities of state-of-the-art machine learning approaches (particularly deep learning) in capturing the underlying physical characteristics of a dynamical system remain poorly understood due to the fact that these algorithms are unable to learn underlying physical features (or characteristics) of the system. Even though some methods for the identification of nonlinear systems seem promising, resulting models often are profligate and lack the convenience of a linear framework description, especially for optimization, optimal and robust control and uncertainty quantification.

An alternative that regained interest in the past decade is the Koopman operator theoretic approach to obtain precise predictions of a nonlinear dynamical system as the output of a truncated linear dynamical system. The main idea behind the Koopman theory [29], [30] is to lift the nonlinear dynamics into a higher dimensional space where the evolution of the flow of the system can be linear. The resulting operator, called Koopman operator, is a linear operator that governs the evolution of scalar functions (the measurements of the nonlinear system). Even though the

core challenge of the Koopman operator theoretic approach is to specify (directly or indirectly through decompositions) the Hilbert space of measurement functions of the state of the system, the theory has been applied for uncontrolled [31], [32] and controlled systems [33], [34] with promising results using popular subspace realization methods such as ERA or Dynamic Mode Decomposition (DMD) and its extensions [35]. The resulting linear operator is a local approximator of the nonlinear dynamical system valid in the neighborhood of a nominal point and the domain of validity of this local linear approximation improves as the dimension of the lifting space is increased. However, one may need a very large dimensional lifting space to accurately capture the flow of the underlying nonlinear system.

In general, one of the alternative to improve the validity region of a linear operator (and curtail the dimension of the lifting space for the Koopman framework) is to consider the linearization of the nonlinear flow about a nominal trajectory of the nonlinear system rather than a nominal point. The linearization about a nominal trajectory leads to a linear time varying (LTV) system as opposed to a linear time invariant (LTI) system for a conventional linear operator. Earliest efforts in the development of methods for linear time-varying systems involved recursive and fast implementations of the time invariant methods by exploring structural properties of the input/output realizations. The classic paper by Chu et. al, exploring the displacement structure in the Hankel matrices is representative of the efforts of this nature. Subsequently, significant results were obtained by Shokoohi and Silverman [36] and Dewilde and Van der Veen [37], that generalized several concepts in the classical linear time invariant system theory consistently. The idea of repeated experiments have been introduced [38], [39] and presented as practical methods to realize the conceptual state-space model identification strategies. However, LTV systems exhibit distinct properties, as compared to the shift invariance exhibited by LTI systems. All the subspace methods for LTI system identification exploit the fact that an infinity of system realizations exist and actually share the same Markov parameters and the eigenvalues of the state transition matrix. However, no such property exists for LTV systems and the lack of similarity transformations handicaps the application of conventional subspace methods to identify LTV systems. In our earlier work [40], [41], it is shown that there actually exists special reference frames, in which the identified models are similar to the true model, i.e., state transition matrices share the same eigenvalues. Using this key result the realizations can be compared across different data sets. This forms the basis for spectral characterization of time-varying systems and the resulting algorithm is known as the time-varying eigensystem realization algorithm (TVERA). In parallel, using an asymptotically stable observer (to remedy the problem of unbounded growth in the number of experiments), a time-varying observer/Kalman-filter system identification (TVOKID) have been implemented to work alongside TVERA.

II. DETERMINISTIC REALIZATION THEORY

In 1965, Ho and Kalman [4] provided a first solution to the challenging system-theoretic problem that became known as the state-space realization problem. It can be stated as follows. Construct a minimal discrete-time state-space realization:

$$\boldsymbol{x}_{k+1} = A\boldsymbol{x}_k + B\boldsymbol{u}_k \tag{1a}$$

$$\boldsymbol{y}_k = C\boldsymbol{x}_k + D\boldsymbol{u}_k \tag{1b}$$

together with an initial state vector $\boldsymbol{x}_0$, where $\boldsymbol{x}_k \in \mathbb{R}^n$, $\boldsymbol{u}_k \in \mathbb{R}^r$ and $\boldsymbol{y}_k \in \mathbb{R}^m$ are the state, control input and output vectors respectively. The constant matrices $A \in \mathbb{R}^{n \times n}$, $B \in \mathbb{R}^{r \times n}$, $C \in \mathbb{R}^{n \times m}$ and $D \in \mathbb{R}^{r \times m}$ represent the internal operation of the linear system, and are used to determine the system's response to any input. The input-output model (or weighting sequence description)

$$\boldsymbol{y}_k = CA^k\boldsymbol{x}_0 + \sum_{i=1}^{k} CA^{i-1}B\boldsymbol{u}_{k-i} + D\boldsymbol{u}_k \tag{2a}$$

introduces the constant matrices sequence

$$h_i = \begin{cases} D & i = 0, \\ CA^{i-1}B & i \geq 1, \\ 0 & i < 0 \end{cases} \tag{3}$$

known as Markov parameters. Essentially, the problem is to replace the infinite description

$$G(z) = \sum_{i=1}^{\infty} h_i z^{-i} \tag{4}$$

with a finite description

$$G(z) = C(zI - A)^{-1}B \tag{5}$$

so that A has minimal dimension. This problem can be divided into two parts, namely, find the degree of $G(z)$ (which is then the minimal dimension of A), and compute the system matrices A, B, C. The Ho-Kalman procedure uses the Hankel matrix for solving this problem, whose factorization into the product of the observability matrix and controllability matrix is given by

$$\boldsymbol{H}_k^{(p,q)} = \begin{bmatrix} h_{k+1} & h_{k+2} & \cdots & h_{k+q} \\ h_{k+2} & h_{k+3} & \cdots & h_{k+q+1} \\ \vdots & \vdots & \ddots & \vdots \\ h_{k+p} & h_{k+p+1} & \cdots & h_{k+p+q-1} \end{bmatrix} \tag{6a}$$

$$= \boldsymbol{O}^{(p)} A^k \boldsymbol{R}^{(q)}. \tag{6b}$$

The fundamental property highlighted by Ho and Kalman is that if the degree of $G(z)$ is n (or the dimension of A is $n \times n$) then $\text{rank}(\boldsymbol{H}_k^{(p,q)}) = n$ and there exist A, B, C of appropriate dimension such that $h_k = CA^{k-1}B$ for $i \geq 1$. The methodology has then been modified and substantially extended to develop the Eigensystem Realization Algorithm (ERA) [9], [10] to identify modal parameters from noisy

measurement data and include data correlations.

Most techniques to identify the Markov parameters sequence Eq. (3) are based on the Fast Fourier Transform (FFT) of the inputs and measured outputs to compute the Frequency Response Functions (FRFs), and then use the Inverse Discrete Fourier Transform (IDFT) to compute the sampled pulse response histories. The discrete nature of the FFT causes one to obtain pulse response rather than impulse response, and a somewhat rich input is required to prevent numerical ill-conditioning. Indeed, the FRF is a ratio between the output and input DFT transform coefficients which requires the input signal to be rich in frequencies so that the corresponding quantity is invertible. However, considerable information can be deduced simply by observing frequency response functions, justifying why FRFs are still generated so often. Another approach is to solve directly in the time domain for the system Markov parameters from the input and output data. In [14], a method has been developed to compute the Markov parameters of a linear system in the time-domain. A drawback of this direct time-domain method is the need to invert an input matrix which necessarily becomes particularly large for lightly damped systems. Rather than identifying the system Markov parameters which may exhibit very slow decay, one can use an asymptotically stable observer to form a stable discrete state-space model for the system to be identified. The method is referred as the Observer/Kalman filter Identification algorithm (OKID) and is a procedure where the state-space model and a corresponding observer are determined simultaneously [15]–[17]. Figure 1 below summarizes the ERA procedure.
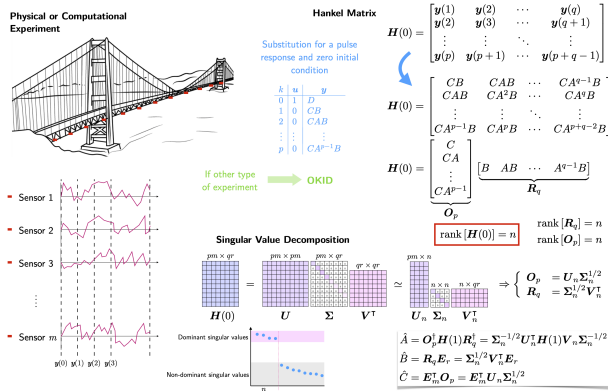

Fig. 1: Illustration of the ERA algorithm

The ERA has occupied the center stage in the current system identification theory and practice owing to its ease, efficiency, and robustness of implementation in several spheres of engineering. Connections of ERA with modal and principal component analyses made the algorithm an invaluable tool for the analysis of mechanical systems. As a consequence, the associated algorithms have contributed to several successful applications in design, control, and

model order reduction of mechanical systems. Because both left and right singular vector matrices of the singular value decomposition are used, ERA yields state space realizations that are not only minimal but also balanced. While the key utility of ERA has been in the development of discrete-time invariant models from input and output experimental data, a consistent computational algorithm could not be formulated for time-varying models because of some gaps in implementing the incomplete theoretical ideas formulated by the researchers in the past. Development of methods for time-varying systems have involved recursive and fast implementations of time invariant methods by exploring structural properties of the input–output realizations [42] or by generalizing several concepts in classical linear time invariant system theory consistently [36], [37]. More recent efforts [43] have concentrated on extending LTI subspace realizations methods by considering moving time windows and weighting factors on the data sequence or introducing explicit parameters to take into account the time-varying amplitude of the corresponding modes during the decomposition phase of the algorithm [44]. However, these efforts suffer from the lack of a method to find similarity transformations between the model sequences for LTV systems obtained from different experimental data sets. For example, the algorithm outlined in [43] is applicable to identify a LTV system from initial condition response data. Mixed experiments, including initial condition and controlled input response experiments, result in identification of different realization, of system matrices at each time. If there were different coordinate systems defined by the Lyapunov transformation $\boldsymbol{w}_k = T_k \boldsymbol{z}_k$ whose state space realization is given by $\boldsymbol{w}_{k+1} = F_k \boldsymbol{w}_k + G_k \boldsymbol{u}_k$, along with $\hat{\boldsymbol{y}}_k = H_k \boldsymbol{w}_k + D_k \boldsymbol{u}_k$, then the realizations A_k, F_k are NOT similar. This is in sharp contrast to the LTI theory, where a variety of realizations (all of infinity of them, that share the same Markov parameters) share the same spectrum. Hence, the lack of a method to find a common reference frame in which different realizations for the LTV system are similar is considered the main drawback of many LTV system identification methods. From a perspective of generalizing the LTI subspace methods to the case of time-varying systems, a time-varying version of ERA has been developed in [40], and it is shown that there exists special reference frames in which the models are similar, i.e., $\tilde{A}_k, \tilde{F}_k$ share the same eigenvalues. This special reference frame can be determined from controllability and observability matrices corresponding to different realizations of the system matrices. Furthermore, an asymptotically stable observer (to remedy the problem of unbounded growth in the number of experiments), a companion algorithm, the time-varying observer/Kalman-filter system identification (TVOKID), has been developed to work alongside with TVERA for the identification of time-varying Markov parameters from experimental data [41].

To get insight into the TVERA process, let us consider

the solution of the difference equation

$$\boldsymbol{y}_k = C_k \Phi_{k,0} \boldsymbol{x}_0 + \sum_{i=0}^{k-1} h(k,i) \boldsymbol{u}_i + D_k \boldsymbol{u}_k \qquad (7)$$

where $\Phi(k, i+1)$ is the state-transition matrix defined as

$$\Phi(k, k_0) = \begin{cases} A_{k-1} A_{k-2} \dots A_{k_0} & \text{for } k > k_0, \\ I & \text{for } k = k_0, \\ \text{undefined} & \text{for } k < k_0. \end{cases} \qquad (8)$$

and $h_{k,i}$ are the generalized Markov parameters (or pulse response matrix) defined as

$$h_{k,i} = \begin{cases} C_k \Phi(k, i+1) B_i & \text{for } i < k-1, \\ C_k B_{k-1} & \text{for } i = k-1, \\ D_k & \text{for } i = k, \\ 0 & \text{for } i > k. \end{cases} \qquad (9)$$

The identification of time-varying system matrices involves the construction of a Hankel matrix $\boldsymbol{H}_k^{(p,q)}$ at each time step consisting of generalized Markov parameters,

$$\boldsymbol{H}_k^{(p,q)} = \begin{bmatrix} h_{k,k-1} & h_{k,k-2} & \cdots & h_{k,k-q} \\ h_{k+1,k-1} & h_{k+1,k-2} & \cdots & h_{k+1,k-q} \\ \vdots & \vdots & \ddots & \vdots \\ h_{k+p-1,k-1} & h_{k+p-1,k-2} & \cdots & h_{k+p-1,k-q} \end{bmatrix}$$
$$= \boldsymbol{O}_k^{(p)} \boldsymbol{R}_{k-1}^{(q)} \qquad (10)$$

where $\boldsymbol{O}_k^{(p)}$ and $\boldsymbol{R}_{k-1}^{(q)}$ are the observability and controllability matrices. The generalized Markov parameters are identified through a least squares process from $\boldsymbol{y}_k$ time histories obtained from forced response experiments using TVOKID [41]. Notice that the rank of the Hankel matrix will be n for a fully controllable and observable system otherwise the rank of the Hankel matrix will be equal to the rank of a completely observable and controllable subspace. The singular-value decomposition (SVD) of $\boldsymbol{H}_k^{(p,q)}$ allows for the identification of the current observability and controllability matrices,

$$\boldsymbol{H}_k^{(p,q)} = \boldsymbol{U}_k \boldsymbol{\Sigma}_k \boldsymbol{V}_k^{\mathsf{T}} \simeq \boldsymbol{U}_k^{(n)} \boldsymbol{\Sigma}_k^{(n)} \boldsymbol{V}_k^{(n)\mathsf{T}} = \boldsymbol{O}_k^{(p)} \boldsymbol{R}_{k-1}^{(q)}$$

$$\qquad (11)$$

$$\Rightarrow \begin{cases} \boldsymbol{O}_k^{(p)} = \boldsymbol{U}_k^{(n)} \boldsymbol{\Sigma}_k^{(n)1/2} \\ \boldsymbol{R}_{k-1}^{(q)} = \boldsymbol{\Sigma}_k^{(n)1/2} \boldsymbol{V}_k^{(n)\mathsf{T}} \end{cases} \qquad (12)$$

where $\boldsymbol{\Sigma}_k^{(n)}$ contains n non-zero singular values of the Hankel matrix and matrices $\boldsymbol{U}_k^{(n)}$ and $\boldsymbol{V}_k^{(n)}$ are constructed from the first n columns of $\boldsymbol{U}_k$ and $\boldsymbol{V}_k$. Finally, the following expression for the identified system matrices are obtained by considering the block shifted Hankel matrices [40]

$$\hat{A}_k = \boldsymbol{O}_{k+1}^{(p)}{}^{\dagger} \boldsymbol{O}_k^{(p)\uparrow}, \ \hat{B}_k = \boldsymbol{R}_k^{(q)}[:, 1:r], \qquad (13)$$

$$\hat{C}_k = \boldsymbol{O}_k^{(p)}[1:n,:], \ \hat{D}_k = h_{k,k}. \qquad (14)$$

Note that $\boldsymbol{O}_k^{(p)\uparrow} = \boldsymbol{O}_{k+1}^{(p)} A_k$ is the block shifted observability matrix.

It is important to note that the Hankel matrix $\boldsymbol{H}_k^{(p,q)}$ cannot be constructed for $k < q$ as the generalized Markov parameters $h_{k,k-q}, h_{k+1,k-q}, \cdots, h_{k+p-1,k-q}$ do not exist. In contrast with the classical formulation of ERA, a second set of experiments (initial condition response experiments) is introduced for the construction of the Hankel matrix for the first few time steps as explained more in details in [40]. Hence, one obtains two sets of realizations for $k < q$ and $k \geq q$. Even though the realized models are topologically equivalent from an input and output standpoint, this does not imply that they are in coordinate systems consistent in time for state propagation purposes. While it is shown in [40] that realizations originating from the same set of experiments are compatible with one another (in other words, the coordinate systems at successive time steps are compatible with one another which makes the model sequences realized useful in state propagation), it is straightforward to see that the initial state given in a certain coordinate system cannot be propagated to the next time step unless the state transition and control influence matrices are expressed in the same (or compatible) coordinate system as the initial state of interest. Any misalignment would cause the state propagation to be physically meaningless and the identified plant model(s) are rendered useless. In essence, system matrices realized for $k < q$ and $k \geq q$ need to be made compatible with one another through a coordinate transformation (isomorphic transformation between successive frames).

Two equivalent realizations A_k and $\hat{A}_k$ are not similar; rather they are topologically equivalent. Topological equivalence (or kinematic equivalence) means that there exists a sequence of invertible, square matrices T_k such that

$$\hat{A}_k = T_{k+1}^{-1} A_k T_k. \qquad (15)$$

Because the system evolution takes place in two different coordinate systems defined by T_k and T_{k+1}, respectively, this leads the basis vectors for the initial time step and the final time step to be different. These frames are defined by left and right eigenvectors of the Hankel matrix during the identification of observability and controllability matrices. Following the development in [40], let us consider $\tilde{\hat{A}}_k$ as the linear transformation of $\hat{A}_k$:

$$\begin{aligned} \tilde{\hat{A}}_k &= \hat{\boldsymbol{O}}_k{}^{\dagger} \hat{\boldsymbol{O}}_{k+1} \hat{A}_k \\ &= T_k^{-1} \boldsymbol{O}_k{}^{\dagger} \boldsymbol{O}_{k+1} T_{k+1} T_{k+1}^{-1} A_k T_k \\ &= T_k^{-1} \underbrace{\boldsymbol{O}_k{}^{\dagger} \boldsymbol{O}_{k+1} A_k}_{\tilde{A}_k} T_k \\ &= T_k^{-1} \tilde{A}_k T_k, \end{aligned} \qquad (16)$$

where $\boldsymbol{O}_k$ is the observability matrix at time k and by virtue of (16), $\hat{A}_k$ and $\tilde{A}_k$ are now similar matrices, i.e, they share the same eigenvalues (Figure 2). One can utilize the observability matrices corresponding to two different identified realizations of the system matrices to define a common frame to predict the system response. In this new frame, the two different realizations are also guaranteed to be similar. This

is a central result for the system identification problem: when the true and identified systems are kinematically similar realizations, the true and identified systems share common eigenvalues after transformation. The same transformation is to be applied for system matrices from different realizations if they originate from different sets of experiments (at time $k = q$ for propagation purposes). Figure 3 summarizes the TVERA procedure.
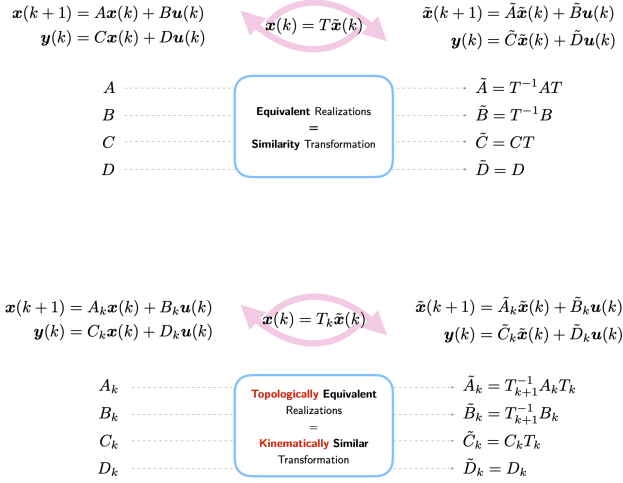

Fig. 2: Illustration of equivalent realizations for LTI vs LTV systems: equivalent realizations for LTI systems are similarity transforms whereas equivalent realizations for LTV systems are kinematically similarity transforms.
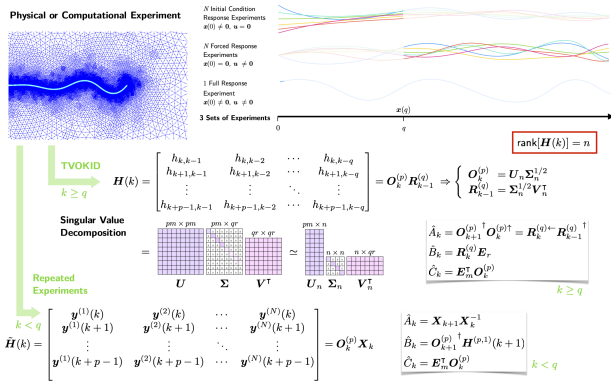

Fig. 3: Illustration of the TVERA procedure

III. NUMERICAL EXAMPLES

This section considers two problems to showcase the utility of the algorithms presented in this paper in predicting the response of a dynamical system. The first benchmark problem, the Duffing oscillator, is declined in of increasing complexity by tuning the parameters

A. Duffing Oscillator

The first example corresponds to the nonlinear oscillator known as the Duffing oscillator governed by following

equations with time-varying coefficients

$$\dot{x} = y, \tag{17a}$$
$$\dot{y} = -\delta(t)y - \alpha(t)x - \beta(t)x^3 + u(t) \tag{17b}$$

Three different cases of increasing complexity are considered corresponding to different dynamics:

1)
   - $\delta(t) = \text{cst} = 0.2$
   - $\alpha(t) = \text{cst} = 1$
   - $\beta(t) = \text{cst} = 0$
2)
   - $\delta(t) = 0.2 + 0.2\sin(2\pi \times 2 \times t)$
   - $\alpha(t) = 1 + 0.5\sin(2\pi \times 3 \times t + \pi/2)$
   - $\beta(t) = \text{cst} = 0$
3)
   - $\delta(t) = \text{cst} = 0.2$
   - $\alpha(t) = \text{cst} = 1$
   - $\beta(t) = \text{cst} = 0.02 \ll 1$

Case 1 corresponds to a linear time-invariant (LTI) system while case 2 is linear time-varying (LTV). Case 3 introduces a slight nonlinearity with $\beta(t) \neq 0$. For identification purposes, data is acquired for 20 seconds at a frequency of 10 Hz. Figures 5d, 5e and 5f show the phase plots displaying the true and identified trajectories while Figures 5a, 5b and 5c show the associated prediction error. As expected, the prediction error corresponding to the case 1 (LTI system) is close to machine precision as we expect perfect reconstruction. Non negligible error is introduced for case 2 as parameters vary in time and the identified model tends to average the oscillations due to variations in $\delta(t)$ and $\alpha(t)$. It is important to mention that the true and identified system matrices for case 1 are related with a similarity transformation (as summarized in Figure 2), hence sharing the same modal properties. This is confirmed by Figure 4 where the eigenvalues of the true and identified A matrices are plotted, matching up to machine precision (absolute error of the order of 10^{-14}).
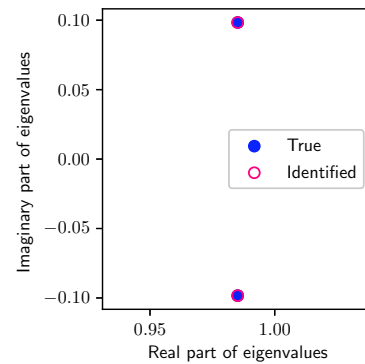

Fig. 4: Eigenvalues of true vs. identified A matrices for case 1

The last case highlights the difficulty to approximate nonlinear dynamics with a LTI model, even when the nonlinearity is small. The error in propagation is now of the order of magnitude of the measured state, invalidating the use of such algorithms for this class of systems.

(a) Phase plot for Case 1   (b) Phase plot for Case 2   (c) Phase plot for Case 3

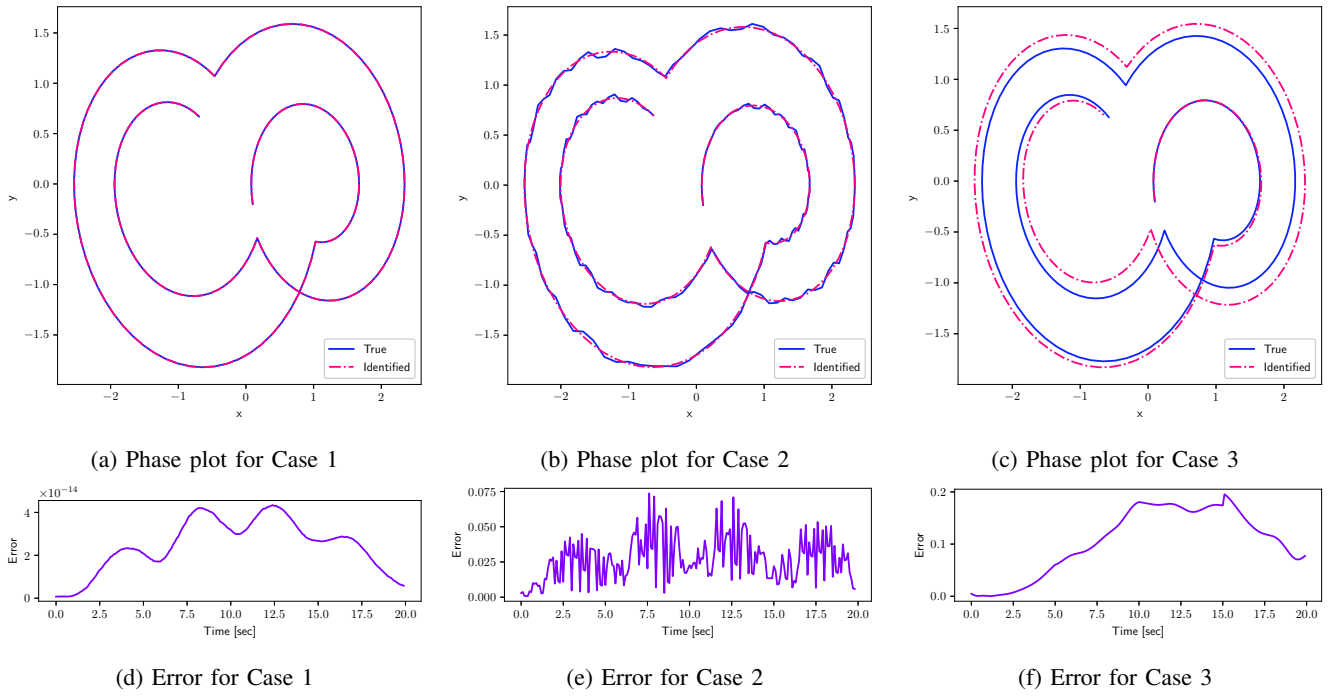(d) Error for Case 1   (e) Error for Case 2   (f) Error for Case 3

Fig. 5: Prediction and error for the Duffing oscillator using ERA.

As explained in the previous section, one can consider a linearization of the nonlinear flow about a nominal trajectory of the nonlinear system rather than a nominal point. The linearization about a nominal trajectory leads to a linear time varying (LTV) system as opposed to a linear time invariant (LTI) system for the conventional ERA. An extension of the ERA algorithm has been developed for the identification of LTV systems in [40], [41] and this section considers utilizes this algorithm to better approximate the time-varying nonlinear dynamics of the Duffing oscillator. For this representative case, it is desired to identify the time-varying linear departure dynamics from a nominal trajectory with initial condition $x_0 = \begin{bmatrix} 0.1 & -0.2 \end{bmatrix}^\top$, input $u(t) = 0.1\text{square}(2\pi t)$ and time-varying coefficients

$$\delta(t) = 0.2 + 0.1\sin(4\pi t) \tag{18a}$$
$$\alpha(t) = 1 + 0.1\sin(6\pi t + \pi/2) \tag{18b}$$
$$\beta(t) = -1 + 0.1\sin(8\pi t + \pi) \tag{18c}$$

The measurement data is recorded at a frequency of 10 Hz for 20 seconds for simulation purposes. A true trajectory is simulated by random sampling of initial deviation from a zero mean Gaussian distribution with standard deviation of 0.05 with deviated input signal $\delta u(t) = 0.1\sin(1.5t)$ for testing purposes. Figure 6a shows the phase plot with the four trajectories: the nominal trajectory, the true trajectory, the identified trajectory and the trajectory from actual linearization of (17) about the nominal trajectory. Figures 6b and 6c display a closer look at the prediction. From these plots, it is clear that the accuracy the time-varying model is superior to a conventional linearization about the initial condition. Table II shows the root mean squared error

(RMSE) averaged over 10 random runs. As expected, the prediction error corresponding to time-varying operator is much better than prediction errors corresponding to any true linearization. These results clearly demonstrates the effectiveness of a time-varying model derived with TVERA.

TABLE I: RMSE for the Duffing departure trajectories

Method	RMSE
TVERA	$3.4 \cdot 10^{-3}$
True linearization	$5.7 \cdot 10^{-2}$

B. Time-varying Koopman operator

This section introduces the time-varying Koopman operator in predicting the response of a nonlinear system. A finite dimension approximation of the infinite dimensional Koopman operator is discussed where polynomial basis functions are considered for the lifting process and time-invariant Koopman operator is also identified to showcase the accuracy gained for the same degree of the lifting process. Considering the exact same dynamics as in Eq. 17 with coefficients described in Eq. 18, the Koopman operator is augmented with polynomial measurements in x and y in three different scenarios:

1) Case 1: Linear basis functions in x and y.
2) Case 2: Basis function up to degree 2 in x and y.
3) Case 3: Basis functions up to degree 3 in x and y.

The measurement data is recorded at a frequency of 10 Hz for 20 seconds for simulation purposes. For this representative case, it is desired to identify the time-varying linear departure dynamics from the nominal trajectory. A nominal trajectory with initial condition $x_0 = \begin{bmatrix} 0.1 & -0.2 \end{bmatrix}^\top$

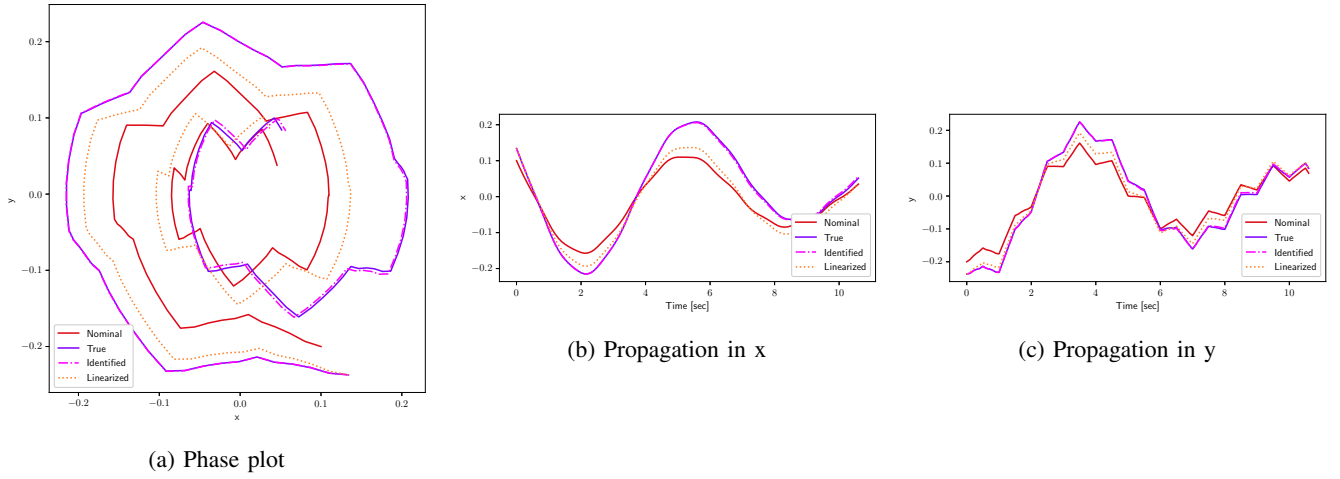(a) Phase plot

(b) Propagation in x

(c) Propagation in y

Fig. 6: Prediction along the nominal for the Duffing oscillator using TVERA.

and zero input is considered. A true trajectory is simulated by random sampling of initial deviation from a zero mean Gaussian distribution with standard deviation of 0.05 with input signal $\delta u(t) = 0.1 \sin(1.5t)$ for identification purposes.

Figure 7a shows the phase plot with the four trajectories: the nominal trajectory, the true trajectory, the identified trajectory and the trajectory from actual linearization of (17) about the nominal trajectory. Figures 7b and 7c show the prediction error corresponding to time-invariant as well as time varying Koopman operator for all the three cases. From these plots, it is clear that the accuracy of the time-invariant as well as time-varying Koopman operators improves with the increase in lifted degree. Furthermore, the time-varying Koopman operator provides at least two order of magnitude better prediction accuracy than the prediction errors corresponding to conventional time-invariant Koopman operator for all the three test cases. While the accuracy of the time-invariant Koopman operator for lifted degree 3, i.e., test case 3 is comparable to actual linearization of the nonlinear flow, the prediction accuracy corresponding to time-varying Koopman operator is five orders of magnitude better than its time-invariant counterpart for lifted degree 3. Finally, Table II shows the root mean squared error (RMSE) averaged over 10 random runs for all the three test cases. As expected, the prediction errors corresponding to time-varying Koopman operator are 3-4 orders of magnitude better than prediction errors corresponding to time-invariant Koopman operator. These results clearly demonstrates the effectiveness of the time-varying Koopman operator as compared to conventional time-invariant Koopman operator.

TABLE II: RMSE for the Duffing departure trajectories

| Lifted space	TI Koopman	TV Koopman
Case 1	$7.5 \cdot 10^{-3}$	$8.8 \cdot 10^{-6}$
Case 2	$6.9 \cdot 10^{-3}$	$2.4 \cdot 10^{-6}$
Case 3	$8.0 \cdot 10^{-4}$	$9.1 \cdot 10^{-8}$
Actual Linearization		$7.1 \cdot 10^{-4}$

IV. CONCLUSION

This paper has introduced a subspace-based identification technique known as the Eigensystem Realization Algorithm (alongside with the Observer/Kalman Idntification Algorithm) to identify discrete time-invariant linear dynamics from I/O data. Two additional algorithms (TVERA and TVOKID) generalize this approach to discrete time-varying linear dynamics and are applied to identify the departure dynamics along a nominal trajectory of a nonlinear dynamical system. Numerical examples based on the Duffing oscillator show the reliability and robustness of these techniques.

REFERENCES

[1] J.-N. Juang, *Applied System Identification*. Englewoods Cliffs, NJ: Prentice Hall, 1994.
[2] O. Nelles, *Nonlinear System Identification: From Classical Approaches to Neural Networks and Fuzzy Models*. Springer Science, 2000.
[3] K. J. Astrom and T. Bohlin, "Numerical identification of linear dynamic systems from normal operating records," *IFAC Proceedings Volumes*, vol. 2, no. 2, pp. 96–111, 1965.
[4] B. L. Ho and R. E. Kálmán, "Effective construction of linear state-variable models from input/output functions," *Regelungstechnik*, vol. 41, no. 2, pp. 545–548, 1965.
[5] T. C. Koopmans, H. Rubin, and L. R. B., "Measuring the equation systems of dynamic economics," *Cowles Comission Monograph*, vol. 10, pp. 53–153, 1950.
[6] E. J. Hannan, *Time Series Analysis*. Methuen, 1960.
[7] E. G. Gilbert, "Controllability and observability in multivariable control systems," *Journal of the Society for Industrial and Applied Mathematics, Series A Control*, vol. 1, no. 2, pp. 128–151, 1963.
[8] R. E. Kálmán, "Mathematical description of linear dynamical systems," *Journal of the Society for Industrial and Applied Mathematics, Series A Control*, vol. 1, no. 2, pp. 152–192, 1963.
[9] J.-N. Juang and R. S. Pappa, "An eigensystem realization algorithm (era) for modal parameter identification and model reduction," *Journal of Guidance, Control, and Dynamics*, vol. 8, no. 5, pp. 620–627, 1985.
[10] J.-N. Juang, J. E. Cooper, and J. R. Wright, "An eigensystem realization algorithm using data correlation (era/dc) for modal parameter identification," *Control Theory and Advanced Technology*, vol. 4, no. 1, pp. 5–14, 1988.
[11] K. F. Alvin and K. C. Park, "Second order structural identification procedure via state-space based system identification," *AIAA Journal*, vol. 32, no. 2, pp. 397–406, 1994.
[12] J.-N. Juang, "Continuous-time bilinear system identification," National Aeronautics and Space Administration, Langley Research Center, Hampton VA, Technical Report, 2003.
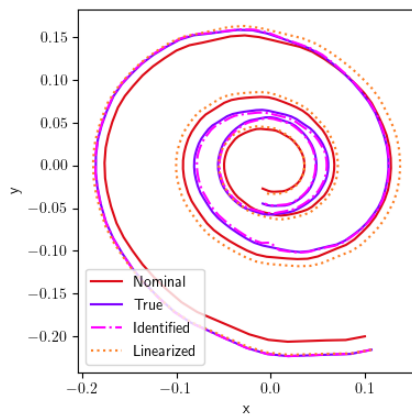
(a) Phase plot for Case 1.
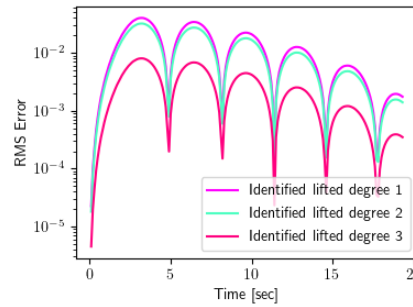
(b) Time-invariant Koopman Operator Approximation.
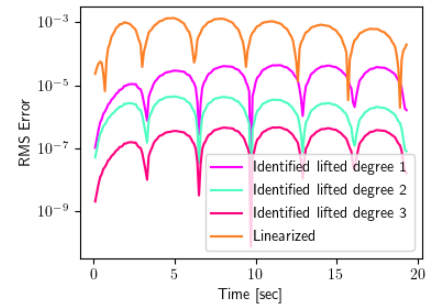
(c) Time-varying Koopman Operator Approximation

Fig. 7: Prediction Error for the Duffing oscillator.

[13] ——, "Generalized bilinear system identification," *The Journal of the Astronautical Sciences*, vol. 57, no. 1 2, pp. 261–273, 2009.

[14] J.-N. Juang, M. Phan, L. G. Horta, and R. W. Longman, "Identification of observer/kalman filter parameters: Theory and experiments," *Journal of Guidance, Control, and Dynamics*, vol. 16, no. 2, pp. 320–329, 1993.

[15] C. W. Chen, G. Lee, and J.-N. Juang, "Several recursive techniques for observer/kalman filter system identification from data," no. 92-4386, Hilton Head Island, SC, U.S.A., 1992.

[16] M. Phan, L. G. Horta, J.-N. Juang, and R. W. Longman, "Linear system identification via an asymptotically stable observer," *Journal of Optimization Theory and Applications*, vol. 79, no. 1, pp. 59–86, 1993.

[17] J.-N. Juang, L. G. Horta, W. K. Belvin, J. Sharkey, and F. H. Bauer, "An application of the observer/kalman filter identification (okid) technique to hubble flight data," 1993.

[18] B. D. O. Anderson and R. E. Skelton, "The generation of all q-markov covers," *IEEE Transactions on Circuits and Systems*, vol. 46, pp. 351–356, 1988.

[19] K. Liu, R. E. Skelton, and J. P. Sharkey, "Modeling hubble space telescope flight data by q-markov cover identification," *Journal of Guidance, Control, and Dynamics*, vol. 17, no. 2, pp. 250–256, 1994.

[20] R. E. Skelton and G. Shi, "Iterative identification and control using a weighted q-markov cover with measurement noise," *Signal Processing*, vol. 52, no. 2, pp. 217–234, 1996.

[21] W. J. Rugh, *Nonlinear System Theory: The Volterra/Wiener Approach*. The Johns Hopkins University Press, 1981.

[22] R. G. Kvaternikm and W. A. Silva, "A computational procedure for identifying bilinear representations of nonlinear systems using volterra kernels," National Aeronautics and Space Administration, Langley Research Center, Hampton VA, Technical Report, 2008.

[23] P. Singla and J. L. Junkins, *Multi-Resolution Methods for Modeling and Control of Dynamical Systems*. Chapman Hall CRC Applied Mathematics Nonlinear Science, 2008.

[24] J. P. Crutchfield and B. S. McNamara, "Equations of motion from a data series," *Complex Systems*, vol. 1, pp. 417–452, 1987.

[25] K. S. Narendra and K. Parthasarathy, "Identification and control of dynamical systems using neural networks," *IEEE Transactions on Neural Networks*, vol. 1, no. 1, pp. 4–27, 1990.

[26] A. U. Levin and K. S. Narendra, "Control of nonlinear dynamical systems using neural networks. ii. observability, identification, and control," *IEEE Transactions on Neural Networks*, vol. 7, no. 1, pp. 30–42, 1996.

[27] S. Haykin, *Neural Networks: A Comprehensive Foundation*. Prentice Hall, 1998.

[28] ——, *Neural Networks and Learning Machines*. Prentice Hall, 2009.

[29] B. O. Koopman, "Hamiltonian systems and transformation in hilbert space," *Proceedings of the National Academy of Sciences*, vol. 17, no. 5, pp. 315–318, 1931.

[30] B. O. Koopman and J.-V. Neumann, "Dynamical systems of continuous spectra," *Proceedings of the National Academy of Sciences*, vol. 18, no. 3, pp. 255–263, 1932.

[31] I. Mezić and A. Banaszuk, "Comparison of systems with complex behavior," *Physica D: Nonlinear Phenomena*, vol. 197, pp. 101–133, 2004.

[32] I. Mezić, "Spectral properties of dynamical systems, model reduction and decompositions," *Nonlinear Dynamics*, vol. 41, pp. 309–325, 2005.

[33] M. Korda and I. Mezic, "Linear predictors for nonlinear dynamical systems: Koopman operator meets model predictive control," *Automatica*, vol. 93, pp. 149–160, 2018.

[34] S. L. Brunton, B. W. Brunton, J. L. Proctor, and J. N. Kutz, "Koopman invariant subspaces and finite linear representations of nonlinear dynamical systems for control," *PLoS ONE*, vol. 11, no. 1, p. e0150171, 2016.

[35] M. O. Williams, I. G. Kevrekidis, and C. W. Rowley, "A data–driven approximation of the koopman operator: Extending dynamic mode decomposition," *Journal of Nonlinear Science*, vol. 25, pp. 1307–1346, 2015.

[36] S. Shokoohi and L. M. Silverman, "Identification and model reduction of time-varying discrete-time systems," *Automatica*, vol. 23, no. 4, pp. 509–521, 1987.

[37] P. Dewilde and A. J. Van Der Veen, *Time Varying Systems and Computations*. Kluwer Academic Publisher, 1998.

[38] M. Verhaegen, *Identification of Time-Varying State Space Models from Input-Output Data*. Workshop on Advanced Algorithms and their Realization, Bonas, 1991.

[39] M. Verhaegen and X. Yu, "A class of subspace model identification algorithms to identify periodically and arbitrarily time varying systems," *Automatica*, vol. 31, no. 2, pp. 201–216, 1995.

[40] M. Majji, J.-N. Juang, and J. L. Junkins, "Time-varying eigensystem realization algorithm," *Journal of Guidance, Control, and Dynamics*, vol. 33, no. 1, pp. 13–28, 2010.

[41] ——, "Observer/kalman-filter time-varying system identification," *Journal of Guidance, Control, and Dynamics*, vol. 33, no. 3, pp. 887–900, 2010.

[42] Y. M. Cho, G. Xu, and T. Kailath, "Fast recursive identification of state space models via exploitation of displacement structure," *Automatica*, vol. 30, no. 1, pp. 45–59, 1994.

[43] H. Zhang, C. W. Rowley, E. A. Deem, and L. N. Cattafesta, "Online dynamic mode decomposition for time-varying systems," *SIAM Journal on Applied Dynamical Systems*, vol. 18, no. 3, pp. 1586–1609, 2019.

[44] T. Sayadi, P. J. Schmid, F. Richecoeur, and D. Durox, "Parametrized data-driven decomposition for bifurcation analysis, with application to thermo-acoustically unstable systems," *Physics of Fluids*, vol. 27, no. 3, p. 037102, 2015.